Limnol. Oceanogr., 43(3), 1998, 433–448

Inhibition of marine photosynthesis by ultraviolet radiation: Variable sensitivity of phytoplankton in the Weddell–Scotia Confluence during the austral spring

Patrick J. Neale
Smithsonian Environmental Research Center, P.O. Box 28, Edgewater, Maryland 21037

John J. Cullen[1]
Bigelow Laboratory for Ocean Sciences, West Boothbay Harbor, Maine 04575; and Department of Oceanography, Dalhousie University, Halifax, Nova Scotia B3H 4J1

Richard F. Davis[1]
Smithsonian Environmental Research Center

Abstract

To assess the potential impacts of ozone depletion on photosynthesis in the Southern Ocean, we need to know more about effects of ultraviolet radiation (UV) on phytoplankton in Antarctic waters, where, in addition to variable stratospheric ozone, temporal and regional differences in vertical mixing might influence photosynthesis and photoacclimation of phytoplankton assemblages. Toward this end, we quantified the responses to UV of Antarctic phytoplankton in the Weddell–Scotia Confluence during the austral spring of 1993. Experimental results on spectral sensitivity of photosynthesis were fit statistically to a model that incorporated uninhibited photosynthesis as a function of photosynthetically available radiation (PAR), wavelength-dependence of inhibition, and the kinetics of photosynthesis during exposure to UV. In contrast to previous results on UV-induced photoinhibition in a diatom culture at 20°C, natural phytoplankton from open waters of the Antarctic showed no ability to counter UV-induced inhibition of photosynthesis during exposures of 0.5–4 h: the rate of photosynthesis declined exponentially as a function of cumulative exposure, and inhibition was not reversed during incubations for up to 3.5 h under benign conditions. The results suggest that nonlinear exposure–response relationships are necessary for modeling UV-dependent photosynthesis in the surface mixed layer of the springtime Weddell–Scotia Confluence. Consequently, we modified our laboratory-based model of photosynthesis and photoinhibition to describe photoinhibition as a nonlinear function of biologically weighted cumulative exposure to damaging irradiance. The model described ~90% of the spectrally dependent experimental variation in photosynthetic rate, and yielded six biological weighting functions (BWFs) for phytoplankton in the Weddell–Scotia Confluence. Assemblages from different stations showed substantial variability in sensitivity to UV. Tolerance of UV was generally highest in assemblages from shallower mixed layers, which presumably had experienced higher irradiance, including UV, prior to sampling. The BWFs of assemblages that seemed acclimated to low irradiance showed the highest sensitivity to UV yet seen for Southern Ocean phytoplankton. The pattern of UV sensitivity was consistent with acclimation, but also with selection against less tolerant species.

Stratospheric ozone depletion has focused efforts on determining the effects of solar ultraviolet radiation (UV, 290–400 nm) on phytoplankton photosynthesis, especially in the Southern Ocean. During the austral spring (October–November), chlorine chemistry within the Antarctic polar vortex results in complete destruction of ozone within much of the middle stratosphere and a >50% decrease in total column ozone (Solomon 1988). Springtime depletion of ozone within the polar vortex (the "ozone hole") has become increasingly widespread, and now encompasses large portions of the Southern Ocean (WMO 1995; Hofmann 1996).

Ozone depletion results in wavelength-dependent changes in solar ultraviolet-B (UVB, 290–320 nm) penetrating the atmosphere. In order to quantify the biological effects of those changes, wavelength-dependent weighting functions are required (Caldwell et al. 1986; Coohill 1989). Any description of spatial or temporal changes in biologically effective UV involves a weighting function, either implicitly or explicitly (Cullen and Neale 1997). Choice of the biological weighting function (BWF) can have an overriding influence on the prediction of relative biological effects (Rundel 1983; Booth and Madronich 1994; Coohill 1994).

During the past decade, much has been learned about the influence of UV and ozone depletion on phytoplankton photosynthesis in the Southern Ocean. Several field experiments have been conducted in which photosynthesis was measured over several hours under natural photosynthetically available

[1] Present address: Center for Environmental Observation Technology and Research, Department of Oceanography, Dalhousie University, Halifax, Nova Scotia B3H 4J1.

Acknowledgments

We thank other members of the science team, officers, and crew of the *Nathaniel B. Palmer* 1993 Weddell–Scotia Cruise (NBP93-6), Antarctic Support Associates support personnel, and staff of the Agencias Universales S.A. for sampling assistance and logistics support. We thank Charles Gallegos for comments on the manuscript. The research was supported by National Science Foundation grant OPP92-20373 to P.J.N. and J.J.C. J.J.C. acknowledges support from NASA and NSERC Research Partnerships. This is CEOTR publication 11.

radiation (PAR) irradiance (UV excluded), and under parallel treatments screened with one to six different long-pass filters, including progressively greater amounts of first UVA (320–400 nm), then UVB (Helbling et al. 1992; Lubin et al. 1992; Smith et al. 1992; Boucher and Prézelin 1996*a*). The wavelength-dependence of UV-induced photoinhibition was determined by one of two methods (originally described by Rundel 1983): (1) by relating increases of inhibition to incremental exposure for each treatment, e.g. J m^{-2} (Smith et al. 1992; Lubin et al. 1992; Helbling et al. 1992), which then is associated with a characteristic wavelength for the added UV (Lubin et al. 1992; Helbling et al. 1992; *but see* Rundel 1983); or (2) by choosing a general model (e.g. biological effectiveness as an exponential function of wavelength) and statistically fitting model parameters to best describe observed inhibition as a function of average hourly spectral irradiance (Boucher and Prézelin 1996*a*). Somewhat more detailed BWFs for photoinhibition have been determined on natural Antarctic phytoplankton using 72 different controlled exposures (30 min in an incubator) to characterize the interacting influence of UV and PAR on short-term photosynthesis of phytoplankton (Neale et al. 1994). Photosynthetic response was modeled by the combination of a photosynthesis–irradiance (*P–I* curve) with a high-resolution (1 nm) weighting function for the full UV spectrum (the BWF-PI model, Cullen et al. 1992). The shape of the BWF (Neale et al. 1994) and overall sensitivity to UV inhibition (Neale et al. 1994; Vernet et al. 1994) varied between populations from diverse Antarctic environments.

A more general analysis of the BWF for inhibition of phytoplankton photosynthesis by UVB has been described by Behrenfeld et al. (1993). In this study, a BWF for North Pacific phytoplankton was estimated as the exponential function of wavelength that best described inhibition as a linear function of cumulative exposure to weighted UVB. This BWF accounted for 65% of the variation in UVB-dependent inhibition of photosynthesis in diverse assemblages of marine phytoplankton (tropical, temperate, Antarctic). However, these experiments focused on the effects of spectral variation for wavelengths <330 nm. Prediction of relative increases in biological damage associated with ozone depletion requires definition of weights over the full spectral range of biological activity (Quaite et al. 1992); for inhibition of photosynthesis, this range includes UVB, UVA, and, at times, PAR (Cullen et al. 1992).

Biological weighting functions estimated from incubations in the field (low spectral resolution) and laboratory (high resolution) have been used in models to estimate the potential effects of ozone depletion over daily or seasonal time scales (Holm-Hansen and Helbling 1993; Arrigo 1994; Boucher and Prézelin 1996*b*). These models extrapolate effects from the incubation time-scale and require explicit description, or at least implicit assumption, of the temporal-dependence and reciprocity of UV effects. Reciprocity is satisfied when the effect of a total radiation exposure (e.g. J m^{-2} weighted appropriately) is independent of the exposure rate (weighted W m^{-2}; *see* Smith et al. 1980; Cullen and Lesser 1991); that is, inhibition is a function solely of cumulative exposure. Reciprocity has been assumed when measurements made over different periods are plotted together and described analytically as a function of cumulative exposure (e.g. Behrenfeld et al. 1993; Smith et al. 1992). Because mean irradiance and cumulative exposure can covary, a separate analysis is required to test for reciprocity. Behrenfeld et al. (1993) tested for reciprocity by plotting inhibition as a function of weighted irradiance ("dose-rate") in incubations conducted on different days in the North Pacific. Results were consistent with a dependence of inhibition on cumulative exposure, but they did not conclusively support or reject reciprocity. Time-series measurements of UV-induced inhibition of photosynthesis at a constant dose rate are a more direct test of reciprocity. This approach has been applied to laboratory cultures of a marine diatom growing at 20°C, which were exposed to different constant intensities of supplementary UVB radiation for periods up to 4 h (Cullen and Lesser 1991). The rate of photosynthesis declined in response to UVB, and within ~30 min reached a rate that decreased no further for the remainder of the experiment, despite continued exposure to UVB. Thus reciprocity failed, supporting the assumption that the inhibition of photosynthesis by UV could be described as a function of biologically weighted irradiance (i.e. the BWF-PI model, with weightings, $\varepsilon(\lambda)$, having units of reciprocal W m^{-2}; *see* Cullen et al. 1992). The extent to which Antarctic phytoplankton can attain a balance between UV damage and counteracting recovery processes during UV exposure on minutes–hours time-scales is unknown. Nevertheless, reciprocity of UV effects has been implicitly assumed in some models of Antarctic primary productivity (Helbling et al 1992; Prézelin et al 1994) but not in other, irradiance-dependent models (Arrigo 1994; Boucher and Prézelin 1996*b*).

When studying the effects of ozone depletion on Antarctic phytoplankton, it is useful to focus on locations and times when the influence of the ozone hole is greatest (Smith et al. 1992), but other factors also need to be considered. The absolute effect of ozone depletion on Antarctic phytoplankton production depends on both the amount of ice cover and presence of significant phytoplankton biomass during the early austral spring (i.e. October–November) (Helbling et al. 1994). The highest biomass in the Southern Ocean is associated with receding marginal ice zones (Smith and Nelson 1986), other frontal regions (Bianchi et al. 1992; de Baar et al. 1995), and coastal areas (Holm-Hansen and Mitchell 1991). The Weddell–Scotia Confluence (WSC) is an example of a frontal region where the cooler, fresher water from the surface of the northern Weddell Sea flows north through passages of the Scotia arc over the warmer, but saltier, water of the Scotia Sea (Bianchi et al. 1992; Muench et al. 1992). This complex hydrographic regime favors high phytoplankton growth in the early spring as documented by oceanographic data (Nelson et al. 1987) and CZCS images for the region (Sullivan et al. 1988; Comiso et al. 1990).

In October–November 1993, diverse studies were conducted on the photobiological and photochemical effects of UV in the WSC. Here we report on the biological weighting functions for UV inhibition of photosynthesis of the WSC assemblages. We show that UV inhibition was a nonlinear function of cumulative exposure to UV and that BWFs of WSC phytoplankton varied in time and space, consistent with inferred light history of phytoplankton assemblages.

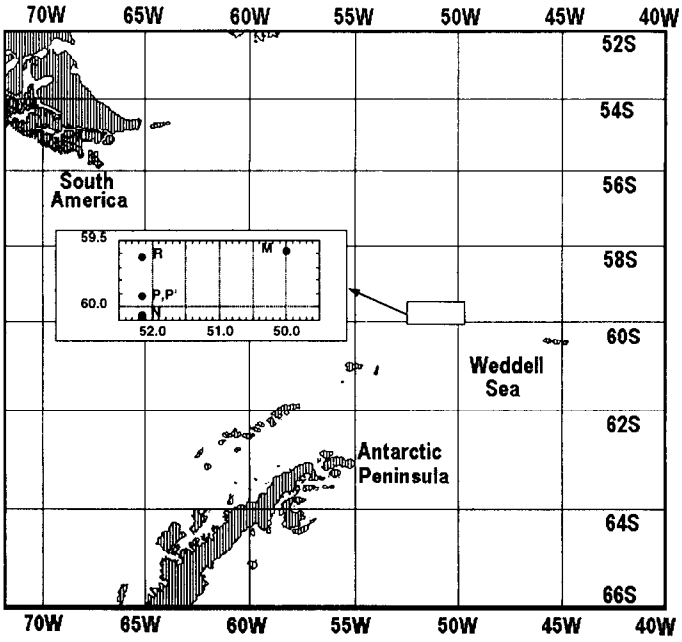

Fig. 1. Station locations in the Weddell–Scotia Confluence during October–November 1993. Inset shows the positions of stations used for photobiological experiments and water column profiles. Stations P, P′, and R were the primary sampling stations for measurements of biological weighting functions.

The variability of BWFs and time-dependence of inhibition must be taken into account to model the effect of increased UV during ozone depletion on primary productivity in the Southern Ocean.

Study area

Phytoplankton populations were sampled during the austral spring of 1993 (10 October–10 November) in the WSC near 60°S, 51°W, about halfway between Elephant Island and South Orkney Island. Photosynthesis measurements were performed at four primary stations (M, N, P and R) occupied between 24 October and 7 November (Fig. 1). At each station, depth profiles between 0 and 200 m were obtained with measurements of conductivity, temperature, density (σ_t) (SeaBird 911 with SeaSoft), chlorophyll fluorescence (Chelsea Instruments), and beam attenuation (SeaTech transmissometer, 0.25-m pathlength). The data were averaged in bins of 1-m depth increment.

Materials and methods

Samples for photosynthesis measurements were normally taken with 12-liter (General-Oceanics, Go-Flo) Niskin bottles attached to a CTD-rosette. On 30 October and 2 November the rosette could not be deployed due to rough seas, and samples were obtained with a clean plastic bucket. Depth profiles of UV irradiance were measured with a Biospherical Instruments PUV-500 radiometer that had five channels with nominal band width of 10 nm (FWHM) and effective center wavelengths of 304, 318, 344, and 384 nm (Kirk et al. 1994). Routine samples were taken early morning (4 h before local noon, except 30 October, 5 h before local noon) from the surface mixed layer at a depth of 15–20 m (i.e. at or below the depth at which irradiance in the 304-nm channel was <1% of surface incident). Chlorophyll *a* concentration (Chl) was measured fluorometrically (Turner Designs Model 10–005R) on aliquots concentrated on glass-fiber filters (Whatman GF/F) and extracted in 90% acetone for at least 24 h in the dark. For determination of BWFs a spectral incubator (the "photoinhibitron") was used essentially as previously described (Cullen et al. 1992; Neale et al. 1994). The incubator consists of an aluminum block plumbed for coolant flow, with 72 sample holes that provide nine irradiances (neutral-density filters) for each of eight Schott long-pass filters with different cutoff wavelengths in the UV (WG series 280, 295, 305, 320, 335, 345, 360, and GG395; *see* Cullen et al. 1992, fig. 2). The shortest wavelength with measurable irradiance was 282 nm (WG280 and WG295 filters). Sample aliquots (2 ml) in cuvettes with flat quartz bottoms are irradiated with a 1,000-W xenon-arc lamp (Oriel) that is directed upward to the bottom of the block by a UV-reflecting/IR-transmitting mirror and then through a 5-cm water/glycol heat filter. Temperature during photoinhibitron incubations was maintained between −1.0°C and 0°C. The uptake of [^{14}C]bicarbonate into organic compounds was measured over a 1-h incubation period. In a variation of the protocol to measure time-dependence of photosynthetic rate, three successive incubations were conducted using the same sample. The first incubation was 0.5 h, the second 1 h, and third 2 h long, with about 15-min change-over period in between. Only four of the photoinhibitron filters were used (WG series 280, 295, 305 and 320), resulting in a total of 36 measurements per incubation. In all cases, at the end of the incubation 0.2 ml of 10% HCl was added to each cuvette. The cuvette contents were emptied into a 7-ml scintillation vial, as were two rinses with 0.1 ml of filtered seawater. The vials were shaken overnight, after which 4 ml of Ecolume scintillation cocktail was added and the samples were counted on a Beckman 3801 liquid scintillation counter with SQPI protocol.

We made a further modification of the method to work with the highly aggregated phytoplankton that were encountered in the WSC. The assemblages were dominated by the diatoms *Thalassiosira gravida* and *Chaetoceros tortissimus* (Irene Schloss pers. comm.), which were mainly in the form of large (sometimes >1 cm) colonies. Such large and relatively rare (<100 liter^{-1}) colonies were incompatible with the small working volume (2 ml) of the photoinhibitron approach. Therefore, samples were gently homogenized at 0°C in batches of 20–30 ml using a Teflon pestle in a glass homogenizer that was cleaned with Micro detergent (Cole-Parmer) and thoroughly rinsed with Nanopure water and sample water to minimize possible toxic effects. Care was taken to use uniform procedures in handling all samples, including keeping samples on ice and driving the Teflon pestle at a consistent slow speed with a motorized drill. The total number of photosynthesis measurements for each BWF was also increased by conducting two successive 1-h incubations using two subsamples from the same Niskin cast. Sample for the second incubation was stored in the dark

(0°C) in a clean polycarbonate bottle, and homogenized immediately before the assay. In the sequential incubation experiment, sample was homogenized before the 0.5-h incubation, the 1-h incubation used the same subsample (stored in the dark on ice), and new subsample was homogenized for the 2-h experiment. Despite homogenization, some samples still contained visible colony fragments, and rates were occasionally more than double the expected rates based on the other samples. Such fragmentation applied to about 10–20 measurements (of a total of 144) per experiment, which were omitted from further analysis.

Larger volume experiments were conducted on intact colonies to assess the effects of homogenization on the spectral-dependence of inhibition. For these experiments, sample water in six rectangular quartz cuvettes (80 ml) was exposed to irradiance from a xenon lamp transmitted through either Schott long-pass glass filters (WG series 280, 295, 305, 360, and GG395) or mylar (nominal 50% cutoff, 315 nm). The quartz cuvettes were immersed in a seawater temperature bath constructed from UV transparent (UVT) Plexiglas. At the end of the incubation period the cuvette contents were filtered (GF/F) and placed in a 20-ml scintillation vial with 1 ml of 10% HCl. The vials were shaken overnight after which 10 ml of Ecolume was added. The samples were counted to determine incorporation of ^{14}C after shipment of samples to Maryland (~1 month after experiment). Time-course experiments of carbon uptake in homogenized colonies also used this type of incubation; however, optical filtering was accomplished using only UVT, UV opaque (UVO) Plexiglas, neutral-density screens, and blue acetate sheets (as indicated), and total incorporation into duplicate 3-ml subsamples per time-point was determined as for the photoinhibitron measurements.

Spectral irradiance (1 nm resolution) for all laboratory experiments ($E(\lambda)$, W m^{-2} nm^{-1}) was measured with a diode-array spectroradiometer (optical multichannel analyzer, OMA) optimized for UV measurement (Cullen and Lesser 1991). The light collector is a diffuser connected to a quartz fiberoptic cable. The spectroradiometer system was calibrated for absolute irradiance using a NIST-traceable, 1,000-W quartz-halogen lamp operated at 8.00 A (Optronic 83 power supply), and calibrated for wavelength with Hg(Ar) emission lines. All calibrations were made on the ship both before and after laboratory experiments. Spectral irradiance in the photoinhibitron was measured by positioning the collector at the top of the sample well. Measurements of the total (PAR 400–700 nm) using a QSL-100 (Biospherical Instruments) with a 4-π detector (1 cm Teflon ball) were used to determine the correction for the small decrease of irradiance between the top and bottom of the well (~10%). For the experiments with the 80-ml quartz cuvettes, spectral irradiance was measured with the cuvettes dry. Total spectral irradiance during the incubation was obtained by multiplying the dry $E(\lambda)$ by the ratio of scalar PAR in the filled cuvette immersed in the water bath (QSL-100) to 2-π PAR measured with the OMA. For the large-volume cuvettes, weak, but measurable treatment irradiance at wavelengths down to 266 nm were transmitted in the shortest wavelength treatments (WG280, WG295). This was due to the use of thinner Plexiglas and Schott glass filters, and was only discovered after the incubations were done. According to the fitted BWF for the large-volume experiment, treatment irradiance in the 266–282-nm range was <25% of total weighted irradiance in the two shortest wavelength treatments.

Table 1. Symbols and abbreviations.

a_0	Dimensionless	First coefficient for exponential weighting function
a_1, a_2	nm^{-1}	Coefficients for exponential weighting function
a^*_{ph}	m^2 mg Chl^{-1}	Phytoplankton spectral absorbance, chlorophyll-specific
c_i	Dimensionless	Component score of a treatment spectrum for the ith principal component
E^*_{inh}	Dimensionless	Biologically effective fluence rate for inhibition of photosynthesis
$\varepsilon(\lambda)$	$(W\ m^{-2})^{-1}$	Biological weightings for inhibition of photosynthesis as a function of UV irradiance
$\varepsilon_H(\lambda)$	$(J\ m^{-2})^{-1}$	Biological weightings for inhibition of photosynthesis as a function of cumulative exposure to UV
E_{PAR}	W m^{-2}	Photosynthetically available radiation (400–700 nm)
E_{PUR}	W m^{-2}	Photosynthetically utilizable radiation
E_s	W m^{-2}	Characteristic irradiance (E_{PAR}) for saturation of photosynthesis
$H(\lambda)$	J m^{-2}	Radiant exposure
H^*_{inh}	Dimensionless	Biologically effective cumulative exposure for inhibition of photosynthesis
m_i	Dimensionless	Statistically determined weighting factor for component c_i
P^B	$(g\ Chl)^{-1}\ h^{-1}$	Photosynthesis normalized to chlorophyll
P^B_t	$(g\ Chl)^{-1}\ h^{-1}$	Instantaneous rate of photosynthesis at time t
P^B_s	$(g\ Chl)^{-1}\ h^{-1}$	Maximum rate of photosynthesis in absence of inhibition
P^B_{pot}	$(g\ Chl)^{-1}\ h^{-1}$	Potential rate of photosynthesis in absence of inhibition
T	s	Duration of experiment
UV	W m^{-2} nm^{-1}	Ultraviolet irradiance at 280–400 nm
UVA	W m^{-2} nm^{-1}	UV at 320–400 nm
UVB	W m^{-2} nm^{-1}	UV at 280–320 nm

Statistical analysis—We fit the results from the photoinhibitron to a time-dependent model of photosynthesis as a function of UV and PAR irradiance (*see* Table 1 for notations). The general approach is to describe photosynthesis normalized to initial chlorophyll, P^B (g C (g Chl)$^{-1}$ h^{-1}), as the product of a potential rate and an inhibition function:

$$P^B = P^B_{pot} \times f(E^*_{inh}, t). \quad (1)$$

Here, P^B_{pot} is the potential rate in the absence of photoinhibition, and inhibiting irradiance is represented with a dimensionless biologically effective fluence rate, E^*_{inh}, discussed below. Potential photosynthesis is a saturating function of irradiance (Cullen et al. 1992):

$$P^B_{pot} = P^B_s\,(1 - e^{-(E_{PAR}/E_s)}). \quad (2)$$

Here, P^B_s is the maximum potential rate, and E_s (W m^{-2}) is a characteristic value for saturation by PAR, E_{PAR}. Photosynthesis is a function of PAR (Webb et al. 1974); however, it is more realistic to describe P^B_{pot} as a function of photosynthetically utilizable radiation, E_{PUR} (W m^{-2}). Photosynthetically utilizable radiation (Morel 1978) depends on the characteristics of spectral utilization by phytoplankton (Johnsen and Sakshaug 1993) and environmental spectral irradiance, both of which need to be measured or modeled. Our analysis here uses E_{PAR}, and we present a separate estimate of the ratio of E_{PAR} and E_{PUR}.

The second term in Eq. 1, $f(E^*_{inh}, t)$, relates the effect of UV (inhibition) to weighted exposure (exposure response curve, ERC; Coohill 1994; Cullen and Neale 1997). The ERC reflects the dynamics of the response to UV. For the case of temperate phytoplankton cultures, UV exposure on the scale of 1–4 h resulted in a rapid (~15 min) decrease in rates, followed by stabilization at a new, lower steady state that was a hyperbolic function of biologically effective irradiance (Cullen and Lesser 1991). This kinetic behavior is consistent with active repair processes partially counteracting UV damage, such that the steady state is proportional to the function $1/(1 + E^*_{inh})$. (Lesser et al. 1994). Our original BWF-PI model (Cullen et al. 1992) used this hyperbolic function of dimensionless irradiance. In the original model (now referred to as the BWF$_E$-PI model), biologically effective fluence rate, E^*_{inh} (nondimensional), is calculated from weighted spectral irradiance,

$$E^*_{inh} = \sum_{\lambda=280\text{ nm}}^{700\text{ nm}} \varepsilon(\lambda) \times E(\lambda) \times \Delta\lambda. \quad (3)$$

The biological weightings for photoinhibition, $\varepsilon(\lambda)$ (reciprocal W m^{-2}), constitute a BWF similar to an action spectrum (Caldwell et al. 1986; Coohill 1989). An equivalent approach is to specify dimensionless biological weightings and express inhibition as a hyperbolic function of biologically effective (B_{eff}) irradiance, w m^{-2} B_{eff} (Cullen and Neale 1997). We infer $\varepsilon(\lambda)$ given P^B measured under 72 different spectral irradiance treatments in the photoinhibitron. That is, statistically we find the spectral weightings that minimize error in describing effect (inhibition) as a function of weighted exposure, E^*_{inh}.

Because laboratory results cannot be applied uncritically to nature, we checked the kinetics of photoinhibition in the WSC. Our observations (*see below*) contrast strongly with the results from cultures: inhibition was a function of cumulative exposure, not irradiance. Consequently, we chose a response function describing inhibition over 0.5–4 h as a function solely of biologically weighted cumulative exposure. Further consideration of the validity of this assumption is given in the results and discussion sections. If repair is negligible and there is no change in photoprotective processes during the exposure, variation in the instantaneous rate of photosynthesis would be expected to have a simple semilogarithmic relationship with cumulative exposure (i.e. the "survival curve" of Harm 1980). The survival curve relationship is used to construct an equation for the average rate of photosynthesis over the exposure period as follows:

$$\frac{P^B_t}{P^B_{pot}} = e^{-H^*_{inh}} \quad (4a)$$

$$\int_0^T \frac{P^B_t}{P^B_{pot}}\,dt = \frac{P^B_{avg}}{P^B_{pot}} = \frac{(1 - e^{-H^*_{inh}})}{H^*_{inh}} \quad (4b)$$

where H^*_{inh} (dimensionless) is biologically weighted cumulative exposure, P^B_t is the instantaneous rate of photosynthesis at time t, and P^B_{avg} is the average photosynthetic rate for an incubation of duration T. Note that photosynthesis is normalized to initial chlorophyll concentration, so losses of chlorophyll (Prézelin et al. 1994) are not treated separately. Determination of biological weightings for calculating H^*_{inh} is comparable to that for E^*_{inh} in Eq. 3, except that we weight radiant exposure ($H(\lambda)$, J m^{-2}) as

$$H^*_{inh} = \sum_{\lambda=280\text{ nm}}^{700\text{ nm}} \varepsilon_H(\lambda) \times H(\lambda) \times \Delta\lambda, \quad (5)$$

where $H(\lambda) = \int E(\lambda) \times dt$. The weightings, ε_H (reciprocal J m^{-2}), define the BWF for inhibition of photosynthesis. Although in theory the model includes the inhibitory effects of PAR (cf. Cullen et al. 1992), in samples from the WSC we found no evidence of inhibition by PAR in separate measurements of photosynthesis vs. PAR up to 200 W m^{-2} (data not shown; for the period 24 October to 4 November, surface midday PAR [1100–1300 h LT] ranged from 45 to 236 W m^{-2}, with an average of 153 W m^{-2}). Thus, the summation in Eq. 5 was performed between 280 and 400 nm only. The overall model for the average rate of photosynthesis over an incubation is thus:

$$P^B_{avg} = P^B_s(1 - e^{-(E_{PAR}/E_s)}) \times \frac{(1 - e^{-H^*_{inh}})}{H^*_{inh}}. \quad (6)$$

Because radiant energy (H), rather than irradiance (E), is weighted, we refer to Eq. 6 as the BWF$_H$-PI model. This new model of UV- and PAR-dependent photosynthesis is a departure from previous photosynthesis vs. irradiance models (e.g. Platt et al. 1980) in that it explicitly accounts for the nonlinear time-dependence of photoinhibition *during* the incubation (Marra 1978; Neale 1987).

This model provides an analytical basis for the statistical estimation of ε_H given P^B as previously described for the original BWF$_E$-PI model (Cullen et al. 1992; Neale et al. 1994). A detailed protocol for the statistical procedure is given in Cullen and Neale (1997). Briefly, UV spectral irradiance for each treatment, multiplied by the wavelength interval of measurement (1 nm) and normalized to E_{PAR}, was analyzed by principal component analysis. Component scores (the relative contribution of a principal component to a given UV spectrum) were derived for all 72 treatment spectra. Four principal components (PCs, essentially statistically independent shapes) accounted for 99% of the variance of the treatment spectra relative to the mean spectrum. Hence, the spectral shape of a treatment could be described with $z = 4$ scores rather than measurements of $E(\lambda)$ at 114 wavelengths. Biologically weighted cumulative exposure was then expressed as a function of component scores for each treatment:

$$H^*_{\text{inh}} = T \times E_{\text{PAR}} \times \left(m_0 + \sum_{i=1}^{z} m_i c_i \right), \quad (7)$$

where the parameters m_i are the statistically determined weighting factors for the z components, c_i. The weighting m_0 is for the normalized mean spectrum. Multiplication by E_{PAR} restores the magnitude of each treatment. Model parameters (P^B_s, E_s, m_0, and m_i) and standard errors were estimated by nonlinear regression (Marquardt method as implemented by SAS) given measured P^B and initial parameter estimates. The m_i estimated by nonlinear fitting determine the degree to which each PC contributes to the biological effect. The larger the absolute value of m for any component, the stronger the contribution of that component to the BWF. If PCs with large weights for shorter wavelengths contribute strongly to the biological effect, the BWF will likewise have strong weighting at short wavelengths and vice versa. The full BWF ($\varepsilon_H(\lambda)$) is the sum of the weighted contributions from each of the components at each wavelength from 282 to 395 nm.

For every sample, two successive incubations were conducted and a separate P^B_s in Eq. 6 was fit for each incubation. Stepwise regressions (Eq. 6 and 7) were performed, including successively high-order spectral PCs. In all cases, maximum spectral resolution consistent with measurement variability was obtained when two PCs were included; that is, adding additional components (increasing z in Eq. 7) did not significantly increase the fit of the model ($P = 0.05$, F-test; cf. Rundel 1983). Standard errors and parameter correlations of m_i were estimated as part of the nonlinear regression analysis. These errors were then used to calculate the corresponding standard errors and associated confidence intervals for individual ε_H by propagation of errors (Bevington 1969).

A BWF was also estimated by using the results of the 80-ml incubations with intact colonies. These incubations were conducted at saturating irradiance (E_{PAR} of ~60 W m^{-2}), so P^B_{pot} is represented by a the single parameter P^B_s. Also, there were only six spectral treatments, and therefore the PCA method was not attempted. Instead, we used a simpler approach modified from Rundel (1983), in which $\varepsilon_H(\lambda)$ was assumed to follow the equation $\varepsilon_H(\lambda) = \exp(a_0 + a_1\lambda)$. The parameters a_0 and a_1 were then estimated by nonlinear regression, given P^B and measured spectral irradiance (1 nm resolution) in each treatment. Additional fits were performed using a higher order term, i.e. $\varepsilon_H(\lambda) = \exp(a_0 + a_1\lambda + a_2\lambda^2)$, and an intercept term, e.g. $\varepsilon_H(\lambda) = \varepsilon_0 + \exp(a_0 + a_1\lambda)$ (cf. Boucher and Prézelin 1996*a*), but neither of these modifications significantly increased the fit of the model ($P = 0.05$, F-test). Further details on using a modified Rundel method to fit BWF-PI models are given in Cullen and Neale (1997).

Results

Station hydrography—Inhibition of photosynthesis was studied on samples primarily from two stations in the Weddell–Scotia Confluence, P (59.92°S) and R (59.62°S), both at a longitude of 52.16°W (Fig. 1). Vertical profiles at station P on 26 and 27 October 1993 showed a well-mixed surface layer extending to 25–30 m, with a stepped density structure over the remaining upper 200 m (Fig. 2). Phytoplankton biomass, as indicated by fluorescence and beam attenuation, was fairly uniform to 50–70 m, where a sharp density discontinuity occurred and biomass declined (fine-scale variability was associated with phytoplankton colonies). On 28 October there was a sharp increase in westerly winds (from ~10 to 22 m s^{-1}). Isopycnals domed, and both salinity (34.16‰) and density (27.44 σ_t units) showed significant increases in the surface layer prior to the morning sample (0900 h LT). About 2 h later, higher salinity water extended over a mixed layer of ~80 m. The surface water at 0900 h on 28 October had temperature and salinity very similar to water well below the photic zone (i.e. 70–80 m; 1% surface PAR, ~30 m) in earlier profiles (Fig. 3; also see arrows in Fig. 2). This suggests that the surface assemblage on 28 October had a recent deep-water origin and was probably acclimated to low light. Because conditions on 28 October contrasted strongly with the earlier station P samples, we designated the 0900 h sample as Sta. P′. The mechanism of vertical transport (and its associated time-scale) is unknown but is likely coupled to frontal activity, which is typical for this hydrographically complex region (e.g. Muench et al. 1992). The unstable conditions and sharp uplift of isopycnals on 28 October (Fig. 2) indicated proximity to a frontal boundary between two water masses that are evident as two groups in the T–S diagram (Fig. 3).

To avoid the complex frontal region, operations were moved north to Sta. R during 29 October–5 November. During this period, westerly winds continued at 10–15 m s^{-1}, maintaining active and deep vertical mixing. Except for variability from colonies of diatoms, fluorescence and beam attenuation were generally homogeneous over a deep surface layer (~100 m). Depression of fluorescence near the surface was absent or less pronounced. Overall, phytoplankton appeared to be undergoing stronger vertical mixing over a greater depth range at Sta. R as opposed to Sta. P.

Time-dependence of inhibition and recovery—Our test of whether the BWF_E or BWF_H model should be applied to the WSC assemblages is based on the principle of reciprocity—the equivalence of time and intensity of exposure in determining overall response. Reciprocity should only apply over time and intensity ranges for which repair is insignificant (Cullen and Lesser 1991). Operationally, we sought to determine whether inhibition was a function of weighted irradiance (i.e. dose rate) or cumulative exposure (i.e. dose) (Cullen and Neale 1994; Smith and Cullen 1995) with the intention of rejecting one model or the other. Cullen and Lesser (1991) observed inhibition of photosynthesis that was not a function of dose in a temperate diatom in culture. Reciprocity failed and thus repair was considered to be active. Our experiment was a variation on the methodology of Cullen and Lesser (1991). We measured photosynthesis by the Sta. R assemblage over incubations of 0.5, 1, and 2 h using the photoinhibitron with four long-pass filters (*see* materials and methods). The treatment spectra, weighted by the BWF_H for Sta. R (*see* model parameters below), were used to calculate both dose (H^*_{inh}) and relative dose rate (i.e. dose divided by incubation period). We then plotted relative photosynthesis vs. both dose rate and dose, and examined in which case a single curve better described the results over

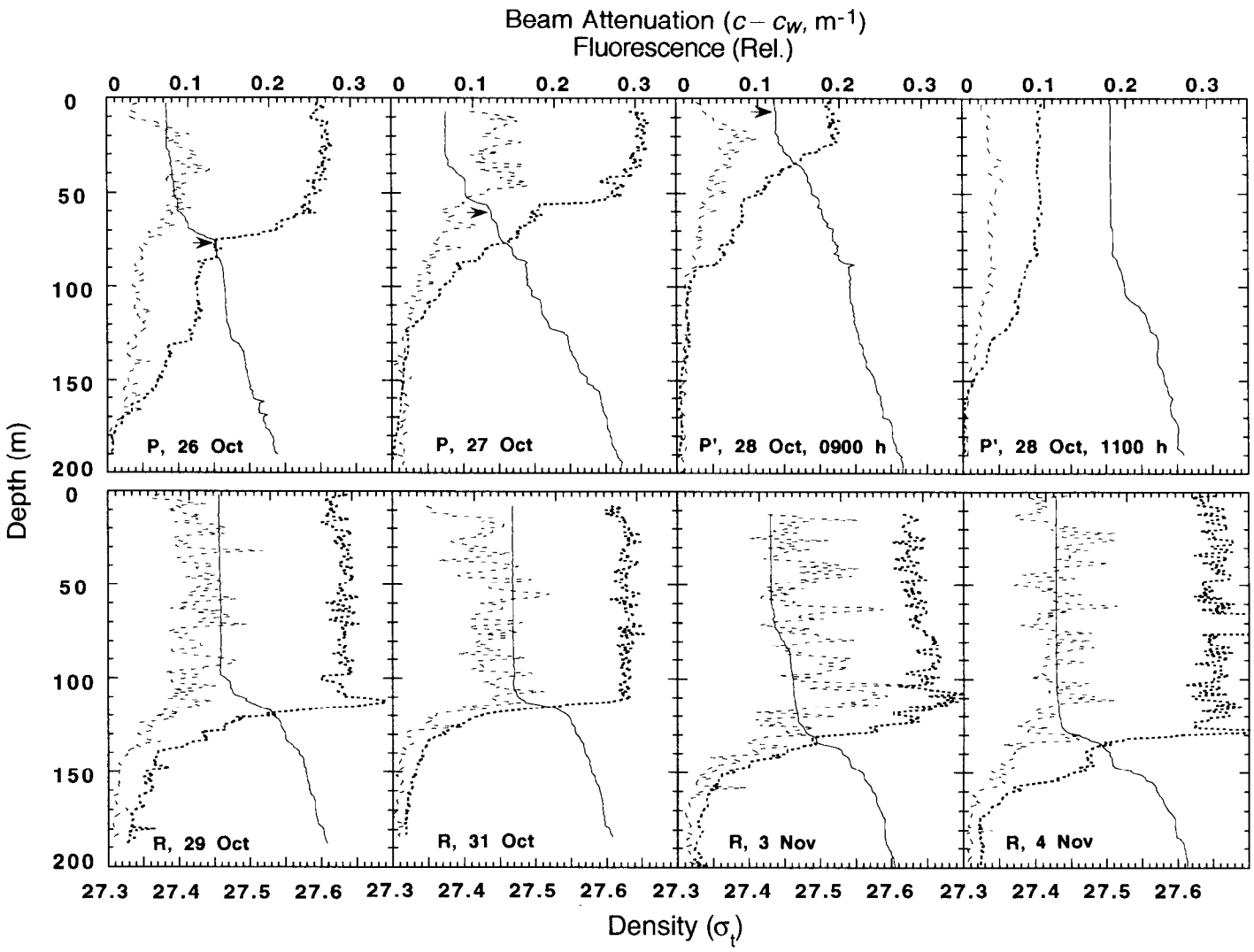

Fig. 2. Vertical profiles of density and phytoplankton parameters for stations in the Weddell–Scotia Confluence during October and November 1993: density (σ_t, solid lines); beam attenuation (c, m^{-1}, corrected for c_w, the contribution from seawater, 0.364 m^{-1}; an indicator of particle concentration, heavy, small dashes); and active Chl fluorescence (light, large dashes). Contrasting conditions were found in the surface layer between the lighter and more stratified waters of Sta. P, which was to the south of the heavier and more strongly mixed waters of Sta. R. Sta. P′ was a frontal station between the two water masses, at which conditions changed rapidly due to increased surface winds. Arrows indicate the 27.44 σ_t isopleth, which moved from 70 m to the surface between P and P′. At Sta. P′, the contrast between an early (0900 h LT) and later (1100 h LT) morning profile shows the rapid deepening of the surface layer.

all incubation times (cf. Cullen and Lesser 1991). The curves for the three incubation times better coincide for the case of the dose response, consistent with a lack of repair processes in the WSC phytoplankton (Fig. 4A,B). The rates are quite variable (especially apparent in the 30-min incubation), which is attributed to residual aggregation in the samples. Nevertheless, the results strongly contrast with the dose-rate dependence observed by Cullen and Lesser (1991) and Lesser et al. (1994) (Fig. 4C,D). However, the differences between the fitted P^B/P^B_{pot} vs. dose-rate curves for different sample times were not statistically significant because of the high variance in rates (Fig. 4A). Therefore, we sought additional experimental evidence to support the dependence of UV inhibition on cumulative exposure.

Another test of the application of the BWF_H-PI model to WSC phytoplankton is whether recovery after UV-induced damage is slow. We examined the kinetics of damage and recovery during time-course measurements of [^{14}C]bicarbonate uptake under inhibiting irradiance, and subsequently under benign, blue-light irradiance (Fig. 5). Photosynthesis was measured during exposure to harmful UVB + UVA + PAR irradiance (UVT) for several hours. Phytoplankton incubated in subsaturating blue light (UVO) served as an uninhibited control. At intervals during the UVT exposure, samples were moved to UVO and measurements of photosynthesis were continued.

As for the sequential incubation (Fig. 4B), results of the ^{14}C time-course experiments (Fig. 5) were consistent with semilogarithmic kinetics of inhibition. Also, we consistently failed to detect any sign of recovery from UV-induced in-

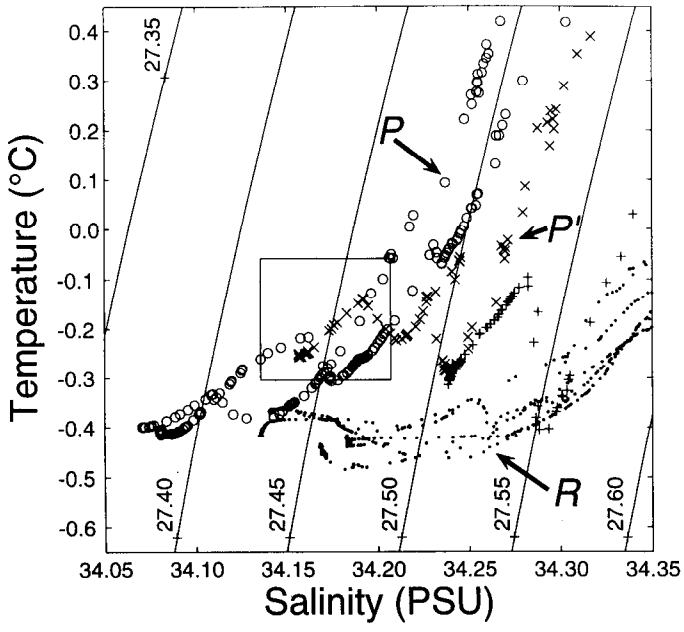

Fig. 3. Temperature–salinity diagram for the upper 200 m of the Weddell–Scotia Confluence for October–November 1993. Profiles are as shown in Fig. 2 with Sta. P (○), Sta. P′ at 0900 h (×), Sta. P′ at 1100 h (+), and Sta. R (●). The diagram is contoured for density at intervals of 0.05 σ_t The inset box delimits water of similar T and S that was at 70–80 m at Sta. P, at the surface at Sta. P′, and not found at station R.

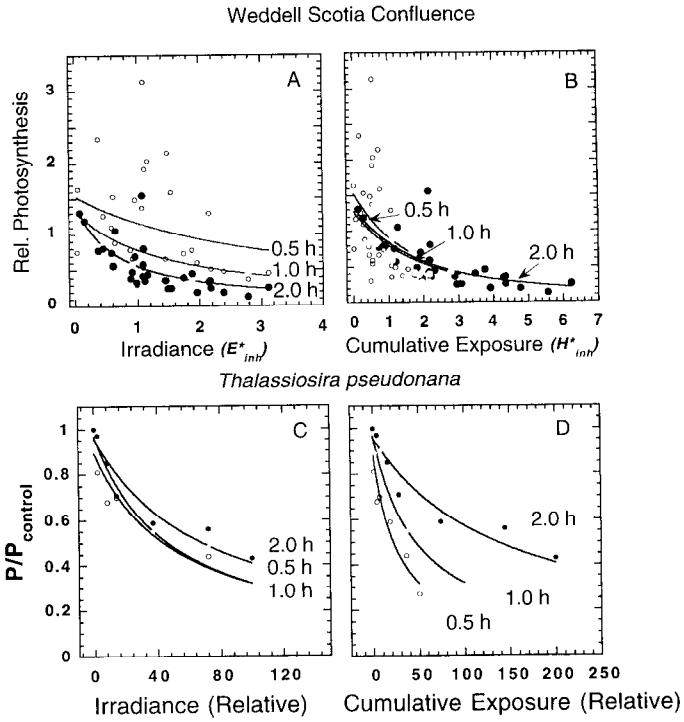

Fig. 4. Testing for reciprocity of UV inhibition of photosynthesis. Cumulative photosynthesis from three consecutive incubations with incubation times of 0.5 h (○), 1 h (▒), and 2 h (●) for samples exposed in the photoinhibitron (WG280, WG295, WG305, or WG320 filters only). Samples were taken on 29 October 1993 (Sta. R). Model estimates of E^*_{inh}, H^*_{inh} and P^B_s for each cell were calculated based on the BWF from 30 October. Relative photosynthesis is the ratio of observed uptake to that predicted in the absence of inhibition (i.e. P^B/P^B_{pot}). PAR was saturating for all points included in the analysis ($E_{PAR} > E_s$). The curves are nonlinear regression fits of relative photosynthesis from each incubation based on (A) a function of dose-rate $[a/(1 + b \times E^*_{inh})]$ or (B) a function of dose, i.e. $a[1 - \exp(-b \times H^*_{inh})]/H^*_{inh}$ (cf. Eq. 4), with a separate a and b fit for each incubation period. For comparison, we also include the data of Cullen and Lesser (1991), which shows the relative photosynthesis of a culture of *Thalassiosira pseudonana* at 20°C under exposure of UV and PAR fluorescent lamps as (C) a function of supplemental UVB irradiance and (D) cumulative exposure. Irradiance is the better predictor of UV inhibition in *T. pseudonana*, but cumulative exposure was the better predictor for the Weddell–Scotia assemblage.

hibition of photosynthesis over the time-scale of several hours; that is, when samples were moved from inhibiting irradiance to benign conditions, the depressed rate of photosynthesis was maintained. Thus, both inhibition and recovery time-series data are consistent with UV effects on photosynthesis being dose-dependent in WSC phytoplankton, at least over time-scales of 0.5–4 h and at high UV irradiance.

Photosynthesis as a function of UV and PAR—During the WSC 1993 cruise, photoinhibitron incubations were conducted on two days at Sta. P, once at P′ and three days at Sta. R. Examples of the photoinhibitron results grouped by spectral treatment are shown in Fig. 6. The maximum contrast was between Sta. P (27 October) and P′ (28 October, 0900 h). The P′ assemblage, presumably transported from depth, was considerably more sensitive to short wavelength UVA and UVB (Fig. 6). In the WG280, 295, 305 and 320 treatments, relative photosynthesis (P^B/P^B_{pot}) at saturating E_{PAR} (>30 W m^{-2}) was 50% lower in the P′ assemblage compared to the P assemblage. At Sta. R, relative photosynthesis in these treatments was intermediate between Sta. P′ and P (data not shown).

Model parameters—The BWF_H-PI model was fit using two replicate incubations conducted using the same morning sample. Overall, the model accounted for ~90% (range 81–94%) of the variance in the mean rate of UV- and PAR-dependent photosynthesis (n = 119–140, Table 2). On 3 d, P^B_s in the second incubation was significantly different from the first incubation, ranging from 20% lower to 40% higher. This could have been due to batch-to-batch differences in the effects of homogenization and diurnal variation of P^B_s (Boucher and Prézelin 1996*b*). On average there was no consistent difference between the first and second incubations. The average P^B_s (0.74 g C (g Chl)$^{-1}$ h^{-1}) is similar to previous reports for Antarctic phytoplankton (Holm-Hansen and Mitchell 1991; *also see* summary of earlier work presented by Cabrera and Montecino 1990), after the effect of homogenization on P^B is taken into account (*see below*). The characteristic irradiance for light saturation, E_s, ranged from 10.2 to 20.1 W m^{-2}, and was lower for assemblages that were presumably acclimated to lower irradiance (Sta. P′ and R), except for the 30 October sample (Table 2). Between-station

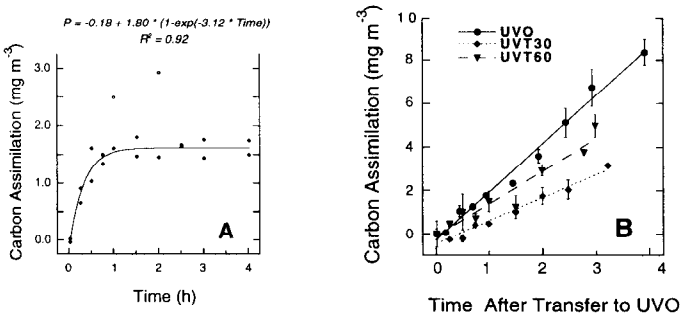

Fig. 5. A. Time-course of UV-induced inhibition of photosynthesis for phytoplankton from the WSC (Sta. R, 6 November 1993). Measurements represent total carbon assimilation in duplicate 3-ml subsamples from an 80-ml quartz cuvette filled with gently homogenized sample labeled with ^{14}C. Illumination was from a xenon lamp transmitted through UVT acrylic and neutral-density screens (~60 W m^{-2} PAR). The curve is a best-fit to a model of dose-dependent inhibition of photosynthesis, with the two high points (open symbols; probably aggregates) excluded. B. Measurements of cumulative photosynthesis after the transfer from UVT to UVO, compared to a control kept in UVO conditions. At intervals (30 min UVT and 60 min UVT are presented here), replicate cuvettes were transferred to UVO irradiance in a backrow of the incubator further screened with blue cellulose acetate and another neutral density screen (~10 W m^{-2} PAR). Completely uniform UVT exposures could not be obtained, and thus the sample exposed to UVT for 60 min was less inhibited during the first hour than the sample shown in panel A. Error bars are the range of duplicates. Initial Chl was 6.4 mg m^{-3}. Similar results were obtained on two other occasions.

differences in E_s, however, were not statistically significant. The average E_s (14.3 W m^{-2} or ~60 μmol photons m^{-2} s^{-1}) is comparable to other indices of light saturation in Antarctic phytoplankton (E_s or I_k) using lamp sources (summary in Cabrera and Montecino 1990), but our E_s is higher than an estimated I_k for in situ incubations (18 μmol photons m^{-2} s^{-1}; Holm-Hansen and Mitchell 1991). One reason for our higher E_s might have been lower photosynthetic utilization of white light in the photoinhibitron as compared to in situ (Harrison et al. 1985). However, using a nominal diatom efficiency spectrum (Johnsen and Sakshaug 1993) we estimate that irradiance in the photoinhibitron would be utilized for photosynthesis with an efficiency fairly close to that in waters with $E_{PAR} \leq E_s$ (i.e. the ratio of PUR : PAR was ~8% lower in the incubator when compared to the water column >15 m; Neale et al. 1998). The proportion of variance in photosynthesis explained by the model (R^2) is lower than previously obtained in culture experiments (Cullen et al. 1992), probably because of the presence of the colonies. Inspection of residuals suggested the model does not systematically over- or underestimate photosynthesis in any of the spectral treatments (e.g. Fig. 6).

All fitted BWFs for UV inhibition of photosynthesis by WSC phytoplankton showed significant inhibitory effect by both UVB and UVA radiation, but absolute sensitivity differed between stations (Fig. 7A). In general, the assemblage sampled at the shallow mixed-layer Sta. P was much less sensitive than assemblages from Sta. P′ and R, which were presumably acclimated to lower exposure. Between Sta. P

proportion over 290–320 nm of 3.5). The difference is tistically significant between 290 and 360 nm (*t*-test, *P* 0.05). Overall, the shape of the BWFs was similar for stations, at least for wavelengths <360 nm. Above 360 the fitted coefficients had different trends with wavelen either dropping sharply (and becoming negative for St on 26 October and Sta. R on 3–4 November) or decrea slowly. However, the ε_H values in five of the six BWF spe are not significantly different from zero over 379–400 (*t*-test, $P = 0.05$). This is consistent with the lack of sig icant inhibition in the P^B vs. E_{PAR} response to long-w length UVA and PAR for both Sta. P (27 October) and P′ (Fig. 6, WG345 and WG360). However, for Sta. P October) ε_H is significantly less than zero for $\lambda > 377$ Negative ε_H values signify that rates of photosynthesis higher when irradiance in those wavelengths was enhan e.g. because of photorepair and(or) photosynthesis (Vin and Roy 1993). Boucher and Prézelin (1996*a*) also repo negative ε at long UVA wavelengths for a coastal ph plankton assemblage sampled near the Antarctic penins

BWF of whole colonies—The photoinhibitron incubat used homogenized samples, so we conducted several ex iments with intact colonies to test whether homogeniza affected the spectral variation in UV sensitivity. Intact s ples (80 ml) were incubated under six spectral treatm and two incubations were conducted on each of two sam from Sta. R (2 and 4 November). The sample on 2 Nov ber was from a bucket, taken from an actively mixing face layer during a storm, and a sample from 20 m was on 4 November. An initial ANOVA of P^B as a functio spectral treatment and sample date showed no consistent ferences between days (*F*-test, $P > 0.2$); therefore, po data were used to estimate a single BWF and P_s^B. In o to estimate a BWF with a low number of spectral treatm we assumed, a priori, that $\varepsilon_H(\lambda)$ is an exponential func of UV wavelength. This approach, first described by Ru (1983), has been recently used to fit BWFs for UV inhib of phytoplankton photosynthesis (Behrenfeld et al. 1 Boucher and Prézelin 1996*a*). We have also shown that tistical analysis of Sta. P and P′ photoinhibitron data u both the Rundel and PCA methods produced BWFs overall similar slopes through the UV (Cullen and N 1997). Thus, our goal in estimating a BWF for the i sample was to determine if there was general consisten the spectral responses of whole and homogenized colo

Photosynthesis by whole colonies at Sta. R was hi variable between experiments in the treatments with U cutoffs (Fig. 8), and thus variance explained by the f model ($R^2 = 0.82$, $n = 24$) was lower than in the ph inhibitron experiments. Photosynthesis was sharply low the 305-nm and shorter cutoff wavelength treatments, was also less variable between experiments (Fig. 8). Ov the whole colonies had low sensitivity to UVA and hi sensitivity to UVB, similar to the results from the disru colonies (Fig. 6). However, disrupted colonies had 35% er P^B, based on the comparison of P_s^B in intact vs. hor enized samples (1.13 vs. 0.74 g C (gChl)$^{-1}$ h^{-1}, $t = 5$

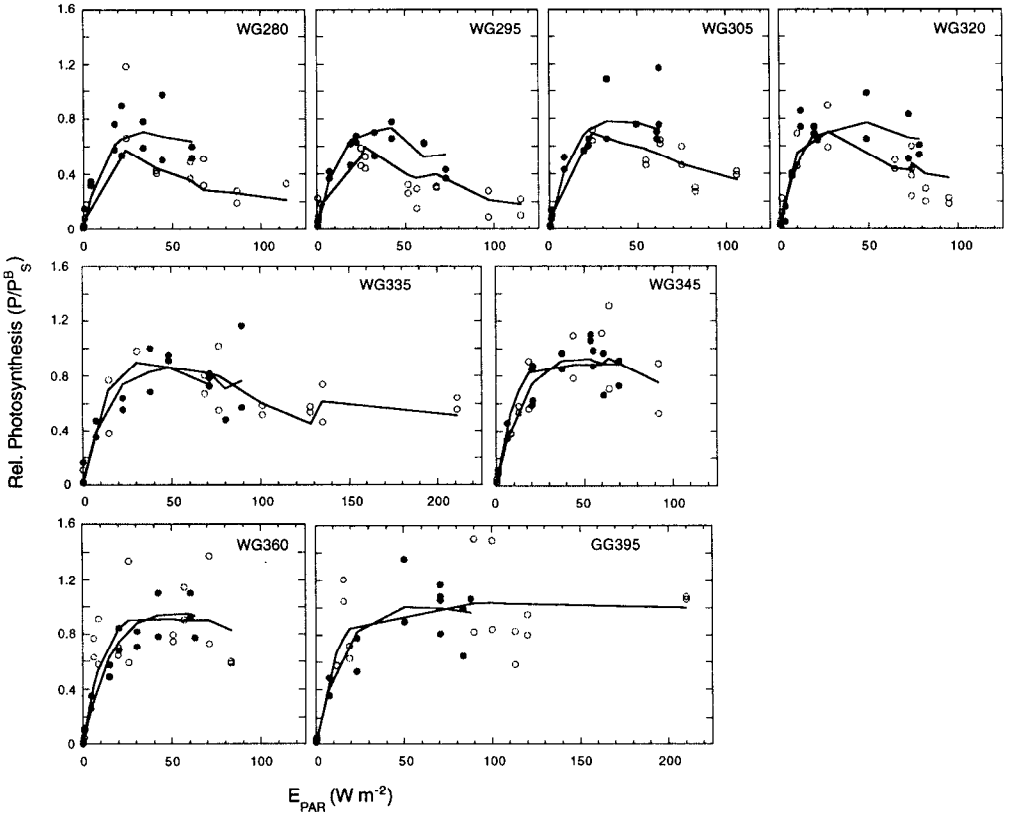

Fig. 6. Photosynthetic response to UV + PAR for phytoplankton from the mixed layer of Weddell–Scotia Confluence Sta. P (●) and P′ (○) sampled on 27 and 28 October 1993, respectively. Each panel shows P^B/P^B_s vs. E_{PAR} for UV + PAR transmitted by one Schott filter (as indicated) at nine intensities (neutral-density screens). Replicate measurements (points) were used to fit the BWF_H/PI model (Eq. 6). Fitted P^B_s was 0.88 (27 October) and 1.1 (28 October) g C (g Chl)$^{-1}$ h^{-1}. Predicted photosynthesis for each treatment is shown, joined by a line. Spectral irradiance varies within the xenon lamp beam, so H^*_{inh}/E_{PAR} differs between cuvettes; thus, there is not a single, smooth *P–I* curve for all points in a spectral group.

Table 2. Summary of the results of statistical analysis of photoinhibition incubations of phytoplankton from the Weddell–Scotia Confluence, 1993. The maximum rate of photosynthesis in the absence of photoinhibition, P^B_s, the characteristic irradiance for the saturation of photosynthesis, E_s, and their respective standard errors (SE) were estimated by nonlinear regression. An average P^B_s is given for cases where a separate P^B_s was fit for each of the two incubations used to estimate the biological weighting function. The coefficient of determination, R^2, was calculated as a proportion of the variance of the mean of the two replicates explained by the BWF_H-PI model. The difference between n and 144 represents the number of measurements not used in the statistical analysis (see materials and methods). The radiation amplification factor (RAF) was calculated by a nonlinear regression fit to the equation $(H^*_{inh})_i/(H^*_{inh})_{300} = (\omega_{300}/\omega_i)^{RAF}$, where $(H^*_{inh})_i$ corresponds to weighted cumulative exposures at the surface using modeled midday irradiance over 1 h calculated at 15 ozone concentrations (ω_i) ranging from 75 to 450 Dobson units, and $(H^*_{inh})_{300}$ is weighted exposure at 300 Dobson units (ω_{300}).

Sta.	Date	$P^B_s \pm$ SE (g C (g Chl)$^{-1}$ h^{-1})	$E_s \pm$ SE (W m^{-2})	$\varepsilon_H(300)$ (J m^{-2})$^{-1}$ $\times 10^4$	R^2	n	RAF
P	26 Oct	1.01±0.15	14.5±3.6	1.36	0.90	134	0.38
P	27 Oct	0.88±0.22	19.0±5.9	0.91	0.93	140	0.18
P′	28 Oct	1.29±0.11	11.7±2.3	3.60	0.89	140	0.23
R	30 Oct	0.63±0.10	20.1±4.5	2.00	0.90	136	0.26
R	3 Nov	0.74±0.09	10.2±2.6	2.61	0.81	119	0.28
R	4 Nov	0.56±0.05	10.5±1.9	2.54	0.88	121	0.30

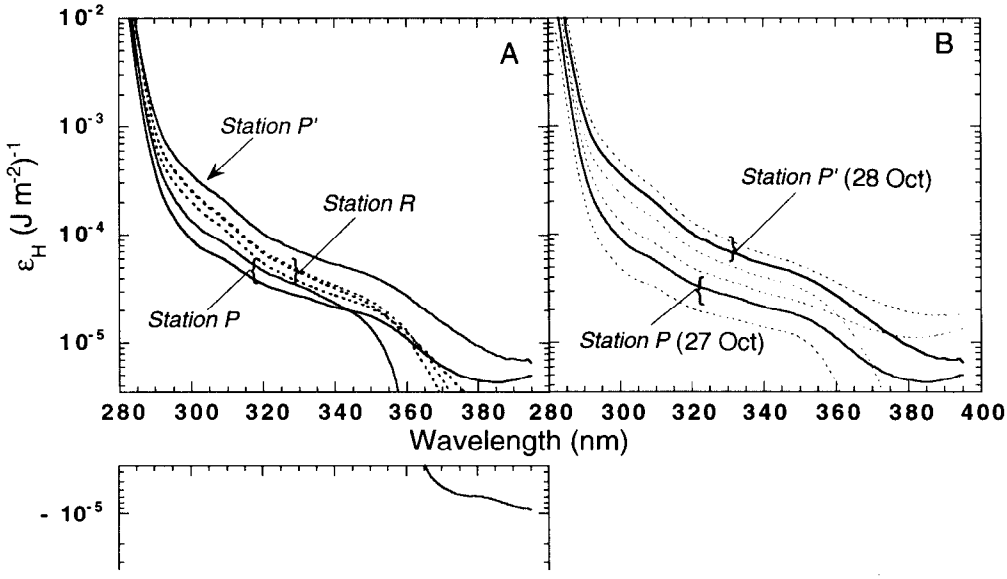

Fig. 7. BWFs for dose-dependent inhibition of photosynthesis (ε_H) based on photoinhibitron measurements in the WSC during austral spring 1993. A. Summary of all BWFs (ε_H) measured for the WSC between 26 October and 4 November 1993, with curves grouped for samples at Sta. P (26–27 October), P′ (28 October), and R (30 October–4 November). The section of the plot below the labels for the *x*-axis shows the range of the BWF of Sta. P, (26 October), over which estimated ε_H are negative. Negative ε_H were also estimated for Sta. R on 3 November ($\lambda > 384$ nm) and 4 November ($\lambda > 378$ nm); however, these weights are all in the range of $-3 \times 10^{-6} < \varepsilon_H < 3 \times 10^{-6}$ and are not statistically different from zero. B. BWFs for samples with maximum (Sta. P′, 28 October) and minimum (Sta. P, 27 October) sensitivity, (base data in Fig. 6), with estimated 95% confidence interval for individual ε_H (dashed line).

tosynthetically inactive cell fragments in the disrupted material.

Using the Rundel method, we estimated a BWF_H with a single exponential slope defined by $\varepsilon_H(\lambda) = \exp(25.2 - 0.107\lambda)$. The estimated BWF_H for whole colonies was similar over the UVB region to the average BWF_H estimated from photoinhibitron data at Sta. R on 3 and 4 November (Fig. 9). In the UVA region, the BWF_H of whole colonies had lower estimated weights than the photoinhibitron BWF_H, but with the high variability in the UVA treatments, the confidence interval for the whole colony BWF_H is very wide. The wavelength range of the whole colony BWF_H extended to 266 nm owing to the presence of shorter wavelengths in the WG280 and WG295 treatments; however, the confidence interval for ε_H overlapped zero below 280 nm since fluxes of experimental irradiance were small. Overall, the single exponential slope in the whole colonies is probably dominated by the response to UV between 280 and 310 nm. In other words, the estimated UVA weights for the whole colonies appear to be significantly lower than for the photoinhibitron BWF, but this could be an artifact of forcing the BWF to have a single slope.

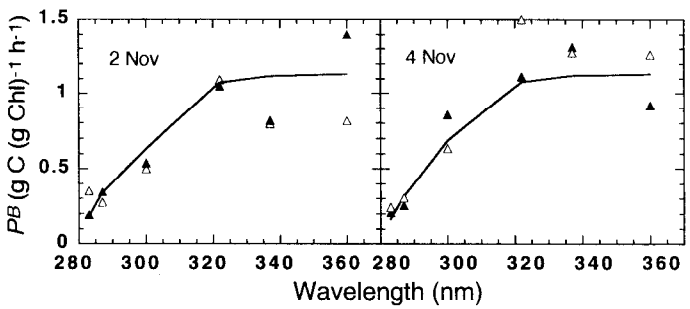

Fig. 8. Photosynthesis of intact samples containing diatom colonies from Sta. R, 2 and 4 November 1993. Samples of 80 ml were exposed in rectangular quartz cuvettes to a xenon lamp filtered by UV long-pass filters (WG280, WG295, WG305, Mylar, WG345, and WG 360) and with PAR sufficient to saturate photosynthesis (~60 W m^{-2}) . Experiments were conducted on two days with two separate incubations on each day (open and filled triangles). Photosynthesis was also predicted with BWF_H/PI model using the BWF for intact colonies (Fig. 9) and P_s^B of 1.13 g C (g Chl)$^{-1}$ h^{-1}. The observed and predicted values are plotted at the wavelength of peak weighted irradiance for each treatment (the maximum of $\varepsilon_H(\lambda) \times E(\lambda) \times \Delta\lambda$).

Discussion

Response to UV exposure—We have shown for phytoplankton from open waters of the Southern Ocean that inhibition of photosynthesis by UV is better described as a function of cumulative exposure than as a time-independent function of irradiance. Such a response is consistent with the absence or very low activity of repair processes counteracting UV damage in these assemblages over time-scales of 30 min to 2 h. At these time-scales reciprocity was well satisfied for the inhibition of photosynthesis by UV. This is in stark contrast to previous results for a diatom culture at 20°C, for

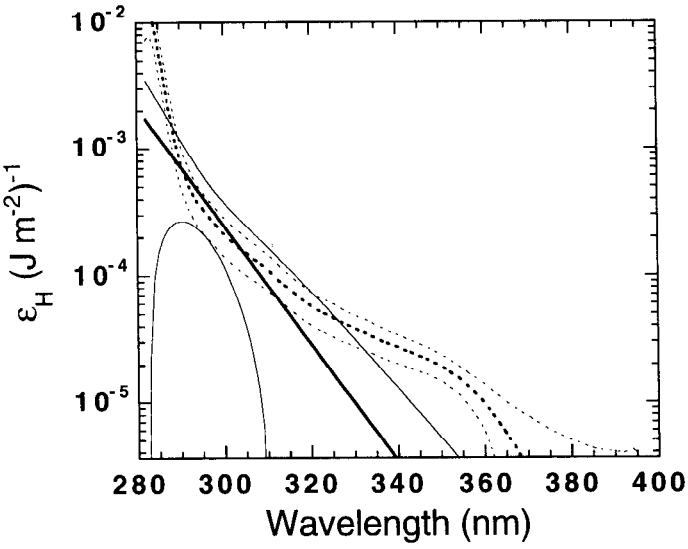

Fig. 9. BWFs for dose-dependent inhibition of photosynthesis (ε_H) for Sta. R (2–4 November 1993) based on incubation of intact colonies (solid lines) vs. photoinhibitron measurements on homogenized samples (dotted lines). Each BWF is shown by a group of three lines—the center heavy line represents $\varepsilon_H(\lambda)$, and the flanking lighter lines are the 95% confidence intervals. The BWF for intact colonies was estimated using data from four incubations of six spectral treatments each. The BWF follows the equation $\varepsilon_H(\lambda) = \exp(25.2 - 0.107\lambda)$ estimated by nonlinear regression ($R^2 = 0.82$; *see* materials and methods). The photoinhibitron BWF is the mean for incubations conducted on 3 and 4 November (Fig. 7), with the confidence interval estimated from the standard error of the mean. The intersection of the lower confidence interval with the *x*-axis indicates the wavelength at which the confidence interval for ε_H overlaps zero.

which reciprocity failed over the same exposure periods and inhibition was best described as function of weighted irradiance. This fundamentally different response demanded a fundamentally different model for describing the relationship between UV exposure and effect (Eq. 4), in which the cumulative effect of inhibition is described as the integral of a semilogarithmic survival curve. In this model, biological weightings, $\varepsilon_H(\lambda)$, have units of reciprocal J m^{-2}, and predicted rates are a function of both exposure time and weighted irradiance.

Similar to our inference of low rates of repair during exposure, our ^{14}C time-course experiments consistently failed to show any sign of recovery from UV-induced inhibition of photosynthesis over the time-scale of several hours (Fig. 5). However (because calibrated irradiance spectra could not be obtained in real time), for many of the samples, the pretreatment inhibition was severe (>50% inhibition in <1 h), including substantial short-wavelength UV. The rate of recovery from milder treatments should also be measured, as should recovery at longer, diurnal time-scales (cf. Smith et al 1992; Prézelin et al. 1994). The rate of recovery after near-surface exposure has a strong influence on whether UV inhibition of water-column production is affected by surface layer mixing (Helbling et al. 1994; Smith and Cullen 1995).

These data from the Antarctic together with our previous results for temperate cultures (Cullen et al. 1992) suggest that in most cases UV inhibition of photosynthesis should have a nonlinear relationship with exposure, although the reason for the nonlinearity varies. When UV response is consistent with our laboratory results (Cullen and Lesser 1991; Lesser et al. 1994), reciprocity fails and inhibition is a hyperbolic function of weighted irradiance (Cullen et al. 1992). On the other hand, if the process is essentially irreversible over the time-scale of damage, photosynthetic rate will decrease as an exponential function of cumulative exposure. For small responses (<50% decrease in average rate over the incubation), the effect will be nearly proportional to exposure (Cullen and Neale 1997). However, for populations that are very sensitive to UV, such as in the WSC, exposure to near-surface conditions (i.e. for >15 min) will significantly decrease the number of susceptible targets in the photosynthetic apparatus. As the latter condition occurs, the decrease in photosynthesis will become noticeably nonlinear (Fig. 4B), consistent with a semilogarithmic survival curve (Harm 1980). It is important to take into account such nonlinearity when applying a BWF to predict the effect of solar UV on the productivity of aquatic ecosystems.

Selection of an appropriate model requires information on both the spectral- and temporal-dependence of UV responses. Goodness-of-fit of a BWF-PI model to data from a *single* time-scale is not diagnostic of which kinetic model applies. Indeed, both the BWF_E and BWF_H models provided acceptable fits (R^2 of ~0.90) to 1-h photoinhibitron data from the WSC (data not shown). Time-course data are required for selecting a model. Finally, both the BWF_E and BWF_H models represent simple cases of a general kinetic model of photoinhibition (Neale 1987; Lesser et al. 1994), and situations may exist where a combination of the two models is necessary, i.e. when repair during exposure is significant but slow.

Differences between stations—There were large differences in sensitivity of assemblages to UV between stations in the WSC, particularly for the 300–320-nm region of UVB. The variation appeared to be systematic as the BWF was stable for much of the period at deeply mixed Sta. R. Overall for Sta. P and R there was much more variation in the overall magnitude of the $\varepsilon_H(\lambda)$ (e.g. absolute ε) compared to the BWF shape (relative proportion of ε at different wavelengths) (Fig. 7); the UV weights for the least sensitive station (P) were more than a factor of 3 lower than the weights for the most sensitive station (P′) (*see also* Cullen and Neale 1997). Because all samples were taken midmorning and incubated near noon, our results strongly suggest that the observed variation in BWFs was due to inherent differences in sensitivity to UV between the assemblages at different stations. Sensitivity could have been lower in the Sta. P assemblages because there was a slower rate of damage, i.e. due to either a smaller absorption cross section or lower quantum yield of damage for the sensitive process. Another possibility is that recovery processes were more active in the more resistant assemblages from Sta. P. We could distinguish between these possibilities through observations on the time-dependence of UV inhibition. However, all such measurements during the WSC 1993 cruise were performed with the

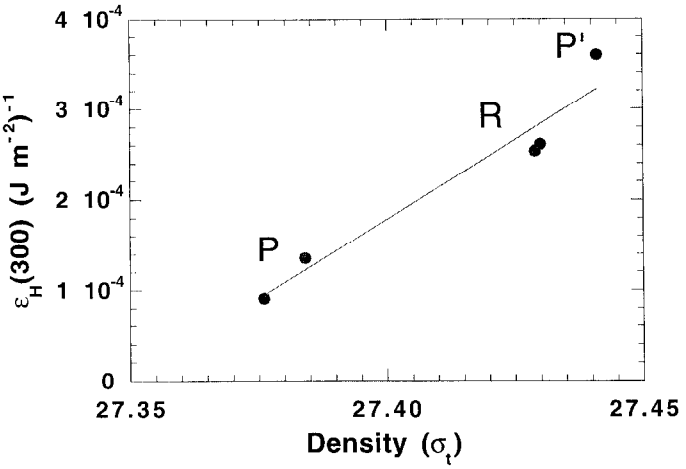

Fig. 10. Correlation between UV sensitivity and hydrography in the Weddell–Scotia Confluence. The BWF_H weight at 300 nm ($\varepsilon_H(300)$) is plotted as a function of sample water density (σ_t), with a line fitted by linear regression ($R^2 = 0.94$). Annotation identifies the station sampled for each BWF. Density was not measured for the bucket sample on 30 October, so it was omitted from the analysis. In this region, higher σ_t in the mixed layer was associated with a greater contribution of deep water (*see* text and Figs. 2 and 3).

high-sensitivity assemblage at Sta. R. Comparative studies of the time-dependence of UV inhibition are needed to better understand the relative contribution of slower rates of damage and enhanced recovery rates to between-assemblage differences in UV sensitivity.

Comparisons between UV sensitivity and other station-specific parameters indicate that variations in UV sensitivity are consistent with acclimation to higher exposure, but also with selection against less tolerant species. In general, Sta. P had a shallower mixed-layer depth than at Sta. R (Fig. 2). The highest sensitivity assemblage (Sta. P′) appears to have had a history of low light exposure at depth. A station parameter that reflects both light history and differences between water mass (and thus mixed-layer phytoplankton assemblages) is density of the surface layer. UV sensitivity (e.g. $\varepsilon_H(300)$) was strongly and positively correlated with surface density (Fig. 10). Pigment analyses by HPLC are also consistent with presumed differences in acclimation state between assemblages. There was a markedly higher concentration of chlorophyllide at Sta. P relative to Sta. R (Anne Sigleo pers. comm). Chlorophyllide is an intermediate in chlorophyll turnover that accumulates in some diatoms. This intermediate may accumulate in late-bloom populations or populations undergoing pigment downregulation due to acclimation to higher irradiance (Ridout and Morris 1985; Jeffrey and Hallegraeff 1987). Therefore, pigment and water density indicate that the Sta. P assemblages were acclimated (or were acclimating) to higher exposure. However, the differences in UV sensitivity between Sta. P and R also coincide with shifts in species composition. At Sta. R, *Thalassiosira gravida* strongly dominated the assemblage, whereas *Chaetoceros tortissimus* dominated at Sta. P (Ferreyra 1995). The presence of UV-absorbing pigments, particularly the mycosporine-like amino acids (MAAs), has also been correlated with resistance to UV exposure in Antarctic phytoplankton (Vernet et al. 1994). A single MAA (probably shinorine) was present in all WSC samples as shown by direct measurements of particulate absorbance (Neale and Spector 1995) and HPLC (Ferreyra 1995). UV absorbance normalized to Chl (e.g. $a^*_{ph}(320)$) was only ~18% lower at Sta. R, as was absorbance at 435 and 670 nm (Table 3). Thus, changes in MAA-mediated photoprotection probably made only a small contribution to changes in UV sensitivity. Our results indicate that both species-specific differences and acclimation to exposure may contribute to differences in UV sensitivity, and studies of the influence of both factors are needed for a comprehensive assessment of UV effects on Antarctic phytoplankton.

Table 3. Averages of hydrographic data for photosynthesis samples at Sta. P and R. Pigment concentrations are from Anne Sigleo (pers. comm.) and phytoplankton absorbance, a^*_{ph}, is from Neale and Spector (1995).

Sta.	Surface density (σ_t)	Chl *a* (mg m^{-3})	Chloro-phyllide *a* (mg m^{-3})	$a^*_{ph}(320)$	$a^*_{ph}(435)$	$a^*_{ph}(675)$
				m^2 mg Chl^{-1}		
P	27.38	0.72	2.43	0.117	0.033	0.022
R	27.43	3.21	0.47	0.098	0.020	0.015

The variation in BWFs between stations in the WSC significantly affects estimates of UV-dependent variation in primary productivity. When integral water-column productivity of the WSC is modeled based on the BWF_H-PI, inhibition associated with UV ranges from <10% to >50%, depending on station and mixing regime (Neale et al. 1998). The WSC BWFs also appear to be significantly different from other, dose-dependent models of inhibition of photosynthesis by UV. For example, a first-order comparison can be made between sensitivity ($\varepsilon_H(300)$) of the WSC assemblages and the overall sensitivity at 300 nm estimated by Behrenfeld et al. (1993) for phytoplankton from diverse environments (in the latter case absolute $\varepsilon_H(300)$ is equivalent to the slope of the dose-response curve). Sensitivity in the WSC ranges from 0.9 to 3.6 × 10^{-4} (J m^{-2})$^{-1}$ compared to 0.7 × 10^{-4} (J m^{-2})$^{-1}$ based on the compilation presented by Behrenfeld et al. (1993; their eq. 4). This further supports the conclusion that WSC assemblages were highly sensitive to UV compared to other marine assemblages; however, the comparison must be considered crude because Behrenfeld et al. (1993) considered all assemblages to have a linear response to cumulative UVB exposure.

Spectral dependence of UV inhibition—Photosynthesis of the WSC phytoplankton assemblages was very sensitive to UVB exposure, compared to UVA. For example, BWFs for the WSC assemblages had a greater relative difference between UVB and UVA than a BWF previously estimated for natural cultures of McMurdo Sound (MCM) diatoms acclimated to high irradiance (Fig. 11; Neale et al. 1994) and a similar proportional decrease in spectral weight from UVB

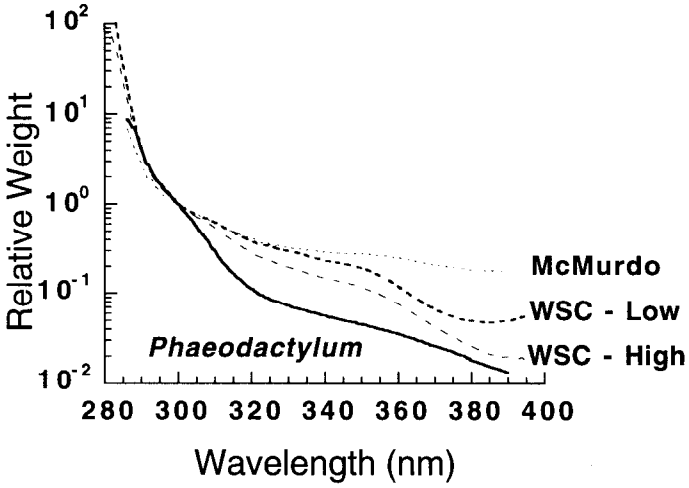

Fig. 11. Comparison of relative spectral weight for UV inhibition of photosynthesis in natural Antarctic assemblages (dashed lines) and in a diatom culture (*Phaeodactylum* sp.) growing at 20°C (solid line). All BWFs are normalized to spectral weight at 300 nm. The Antarctic BWFs were measured using a natural culture of diatoms from McMurdo Sound growing under solar irradiance (Neale et al. 1994) and phytoplankton from the Weddell–Scotia Confluence Sta. P (low sensitivity) and P′ (high sensitivity).

to UVA as for the BWF of a temperate diatom, *Phaeodactylum* sp. (Cullen et al. 1992). Between 290 and 360 nm, biological weight decreases by almost two decades (factor of 100), with the steepest decrease with wavelength occurring in the UVB region. On the other hand, at wavelengths <300 nm, all BWFs had a similar shape (Fig. 11). Comparison between the photoinhibitron and whole-colony BWFs suggests that results of the small-volume incubations are not subject to treatment artifacts and that the strong wavelength-dependence is real. This has implications for the radiation amplification factor (RAF), which is an indicator of the sensitivity of a process to ozone depletion. The RAF is an exponent that describes the relative increase in weighted exposure for a given decrease in ozone (Booth and Madronich 1994), and it depends on the BWF and location (the latter because of sun angle). The RAF calculated for the WSC assemblages, using modeled clear-sky, midday irradiance for the WSC ranges from 0.18 to 0.38 (Table 2). This compares with the RAF for the MCM BWFs of 0.05 (based on McMurdo spectral irradiance; data not shown), and 0.3 for *Phaeodactylum* BWF using midlatitude spectra (*see* review by Smith and Cullen 1995).

Recently, a biological weighting function has been described for UV inhibition of daily average photosynthesis in a surface assemblage from coastal waters of the Antarctic Peninsula (Boucher and Prézelin 1996*a*). The shape of the weighting function (fit using a modification of the Rundel method) shows much lower UVA weights relative to UVB than any other published BWF for UV inhibition of phytoplankton photosynthesis. Accordingly, a much larger RAF (0.91) was calculated compared to the previously described BWFs. However, the Boucher and Prézelin (1996*a*) weighting function addressed changes in daily integrated photosynthesis in relation to daily average spectral irradiance, whereas our weighting function for the WSC assemblage was defined from the cumulative response to 1-h exposures. A relevant basis of comparison between the two BWFs is their prediction of ozone-dependent changes in water column production. Such analyses are presented, respectively, in Boucher and Prézelin (1996*b*) and Neale et al. (1998). Despite the different approaches and shapes of the BWFs, estimates of the effect of 50% ozone reduction on integral primary production are in the same range, <5% for Boucher and Prézelin (1996*b*) and 0.7–8.5% (depending on BWF, assumed mixing regime and cloudiness) for Neale et al. (1998).

The time-scale of measurement in the present study is similar to that used in our previous study of the spectral response to UV in natural cultures of diatoms from McMurdo sound (Neale et al. 1994). In the previous study, the BWF_E-PI model was applied to photosynthesis in the photoinhibitron over a 30-min incubation (not 60 min, as incorrectly reported in Neale et al. 1994). In contrast with the WSC, results indicated that recovery processes were active in the MCM assemblages. Natural assemblages of diatoms were maintained under either UV-exposed (UVT) or UV-protected (UVO) conditions with relatively high PAR. Exposure to solar UV decreased photosynthesis under UVT conditions but, in contrast with the WSC assemblages, photosynthesis recovered upon transfer to UVO conditions (Lesser et al. 1996). The rates in the transfer experiment were close to those predicted using the BWF_E-PI model. Photosynthesis of surface samples from the coastal Antarctic also recovered from exposure to midday solar UV during a 2-h PAR incubation (Boucher and Prézelin 1996*a*). Therefore, the lower sensitivity of the MCM assemblages can be at least partially explained by greater recovery potential, although recovery was insufficient to completely counteract long-term effects of UV exposure. The latter is indicated by the 10% lower P^B in the UVT culture compared to the UVO culture (Neale et al. 1994). The MCM cultures were acclimated to near-surface conditions and were growing rapidly for polar phytoplankton at −1.8°C, i.e. ~0.3 d^{-1}. Phytoplankton growth rates were undoubtedly much lower over the optically deep mixed layers of the WSC; in fact, the mixing depth at Sta. R was probably near or below the compensation level (Nelson and Smith 1991). Thus, polar phytoplankton may not maintain energetically costly UV repair processes when growth rates are very slow because of deep vertical mixing.

No matter what mechanisms are behind the observed differences in sensitivity of Antarctic phytoplankton, some general conclusions may be drawn. First, it is clear that no single BWF applies to all the Weddell–Scotia Confluence, much less all of the Southern Ocean (cf. Behrenfeld et al. 1993; Arrigo 1994; Boucher and Prézelin 1996*a*). Antarctic phytoplankton differ in overall sensitivity to UV and in the relative importance of UVB vs. UVA spectral regions (Helbling et al. 1998; Helbling et al. 1994; Neale et al. 1994). These differences significantly affect estimates of the impact of ozone depletion on primary productivity in the WSC (Neale et al. 1998). Nevertheless, variation in other aspects of the BWF for WSC phytoplankton, such as the shape in the UVB (*see* Behrenfeld et al. 1993), was limited, and variation of

sensitivity to UV was systematic in time and space. Further work on the wavelength-dependence of inhibition and the kinetics of photosynthesis during exposure to UV for Antarctic phytoplankton is needed to establish if these patterns of variation extend over Southern Ocean. As in the WSC, variation of sensitivity to UV may be correlated with hydrography (Vernet et al. 1994) and other photophysiological parameters. With continued efforts, we expect that our understanding of responses to UV will progress in parallel with our understanding of how other photosynthetic characteristics of phytoplankton respond to environmental variability.

References

ARRIGO, K. R. 1994. Impact of ozone depletion on phytoplankton growth in the Southern Ocean: Large-scale spatial and temporal variability. Mar. Ecol. Prog. Ser. **114:** 1–12.

BEHRENFELD, M. J., J. W. CHAPMAN, J. T. HARDY, AND H. I. LEE. 1993. Is there a common response to ultraviolet-B radiation by marine phytoplankton? Mar. Ecol. Prog. Ser. **102:** 59–68.

BEVINGTON, P. R. 1969. Data reduction and error analysis for the physical sciences. McGraw-Hill.

BIANCHI, F., AND OTHERS. 1992. Phytoplankton distribution in relation to sea ice, hydrography and nutrients in the northwestern Weddell Sea in early spring 1988 during EPOS. Polar Biol. **12:** 225–235.

BOOTH, C. R., AND S. MADRONICH. 1994. Radiation amplification factors: Improved formulation accounts for large increases in ultraviolet radiation associated with Antarctic ozone depletion, p. 39–42. *In* C. S. Weiler and P. A. Penhale [eds.], Ultraviolet radiation in Antarctica: Measurements and biological effects. AGU.

BOUCHER, N. P., AND B. B. PRÉZELIN. 1996*a*. An in situ biological weighting function for UV inhibition of phytoplankton carbon fixation in the Southern Ocean. Mar. Ecol. Prog. Ser. **144:** 223–236.

———, AND ———. 1996*b*. Spectral modeling of UV inhibition of in situ Antarctic primary production using a field derived biological weighting function. Photochem. Photobiol. **64:** 407–418.

CABRERA, S., AND V. MONTECINO. 1990. Photosynthetic parameters of the entire euphotic phytoplankton of the Bransfield Strait, summer 1985. Polar Biol. **10:** 507–513.

CALDWELL, M. M., L. B. CAMP, C. W. WARNER, AND S. D. FLINT. 1986. Action spectra and their key role in assessing biological consequences of solar UVB radiation change, p. 87–111. *In* R. C. Worrest and M. M. Caldwell [eds.], Stratospheric ozone reduction, solar ultraviolet radiation and plant life. Springer-Verlag.

COMISO, J. C., N. G. MAYNARD, W. O. SMITH, AND C. W. SULLIVAN. 1990. Satellite ocean color studies of Antarctic ice edges in summer/autumn. J. Geophys. Res. **95:** 481–489, 496.

COOHILL, T. P. 1989. Ultraviolet action spectra (280 to 380 nm) and solar effectiveness spectra for higher plants. Photochem. Photobiol. **50:** 451–457.

———. 1994. Exposure response curves, action spectra and amplification factors, p. 57–62. *In* R. H. Biggs and M. E. B. Joyner [eds.], Stratospheric ozone depletion/UVB radiation in the biosphere. Springer-Verlag.

CULLEN, J. J., AND M. P. LESSER. 1991. Inhibition of photosynthesis by ultraviolet radiation as a function of dose and dosage rate: Results for a marine diatom. Mar. Biol. **111:** 183–190.

———, AND P. J. NEALE. 1994. Ultraviolet radiation, ozone depletion, and marine photosynthesis. Photosynthesis Res. **39:** 303–320.

———, AND ———. 1997. Biological weighting functions for describing the effects of ultraviolet radiation on aquatic systems, p. 97–118. *In* D.-P. Häder [ed.], The effects of ozone depletion on aquatic ecosystems. R. G. Landes.

———, ———, AND M. P. LESSER. 1992. Biological weighting function for the inhibition of phytoplankton photosynthesis by ultraviolet radiation. Science **258:** 646–650.

DE BAAR, H. J. W., AND OTHERS. 1995. Importance of iron for plankton blooms and carbon dioxide drawdown in the Southern Ocean. Nature **373:** 412–415.

FERREYRA, G. A. 1995. Effet du rayonnement UV sur le phytoplancton d'hautes latitudes. Ph.D. thesis, Univ. Québec à Rimouski.

HARM, W. 1980. Biological effects of ultraviolet radiation. Cambridge Univ. Press.

HARRISON, W. G., T. PLATT, AND M. R. LEWIS. 1985. The utility of light-saturation models for estimating marine primary productivity in the field: a comparison with conventional "simulated" in situ methods. Can. J. Fish. Aquat. Sci. **42:** 864–872.

HELBLING, E. W., V. VILLAFAÑE, M. FERRARIO, AND O. HOLM-HANSEN. 1992. Impact of natural ultraviolet radiation on rates of photosynthesis and on specific marine phytoplankton species. Mar. Ecol. Prog. Ser. **80:** 89–100.

———, ———, AND O. HOLM-HANSEN. 1994. Effects of ultraviolet radiation on Antarctic marine phytoplankton photosynthesis with particular attention to the influence of mixing, p. 207–227. *In* C. S. Weiler and P. A. Penhale [eds.], Ultraviolet radiation and biological research in Antarctica. AGU.

HOFMANN, D. J. 1996. The 1996 Antarctic ozone hole. Nature **383:** 129.

HOLM-HANSEN, O., AND E. W. HELBLING. 1993. Polyethylene bags and solar ultraviolet radiation. Science **259:** 534.

———, AND B. G. MITCHELL. 1991. Spatial and temporal distribution of phytoplankton and primary production in the western Bransfield Strait region. Deep-Sea Res. **38:** 961–980.

JEFFREY, S. W., AND G. M. HALLEGRAEFF. 1987. Chlorophyllase distribution in ten classes of phytoplankton: A problem for chlorophyll analysis. Mar. Ecol. Prog. Ser. **35:** 293–304.

JOHNSEN, G., AND E. SAKSHAUG. 1993. Bio-optical characteristics and photoadaptive responses in the toxic and bloom-forming dinoflagellates *Gyrodinium aureolum, Gymnodinium galatheanum,* and two strains of *Prorocentrum minimum.* J. Phycol. **29:** 627–642.

KIRK, J. T. O., AND OTHERS. 1994. Measurements of UVB radiation in two freshwater lakes: An instrument intercomparison. Arch. Hydrobiol. Beih. Ergebn. Limnol. **43:** 71–99.

LESSER, M. P., J. J. CULLEN, AND P. J. NEALE. 1994. Carbon uptake in a marine diatom during acute exposure to ultraviolet B radiation: Relative importance of damage and repair. J. Phycol. **30:** 183–192.

———, P. J. NEALE, AND J. J. CULLEN. 1996. Acclimation of Antarctic phytoplankton to Ultraviolet radiation: ultraviolet-absorbing compounds and carbon fixation. Mol. Mar. Biol. Biotechnol. **5:** 314–325.

LUBIN, D., AND OTHERS 1992. A contribution toward understanding the biospherical significance of Antarctic ozone depletion. J. Geophys. Res. **97:** 7817–7828.

MARRA, J. 1978. Effect of short-term variation in light intensity on photosynthesis of a marine phytoplankter: A laboratory simulation study. Mar. Biol. **46:** 191–202.

MOREL, A. 1978. Available, usable, and stored radiant energy in relation to marine photosynthesis. Deep-Sea Res. **25:** 673–688.

MUENCH, R. D., J. T. GUNN, B. A. HUBER, AND D. G. MOUNTAIN. 1992. The Weddell–Scotia marginal ice zone: Physical ocean-

ographic conditions, geographical and seasonal variability. J. Mar. Syst. **3:** 169–182.

NEALE, P. J. 1987. Algal photoinhibition and photosynthesis in the aquatic environment, p. 35–65. *In* D. J. Kyle, C. B. Osmond, and C. J. Arntzen [eds.], Photoinhibition. Elsevier.

———, R. F. DAVIS AND J. J. CULLEN. 1998. Interactive effects of ozone depletion and vertical mixing on photosynthesis of Antarctic phytoplankton. Nature **392:** 585–589.

———, M. P. LESSER, AND J. J. CULLEN. 1994. Effects of ultraviolet radiation on the photosynthesis of phytoplankton in the vicinity of McMurdo Station (78°S), p. 125–142. *In* C. S. Weiler, and P. A. Penhale [eds.], Ultraviolet radiation and biological research in Antarctica. AGU.

———, AND A. C. SPECTOR. 1995. UV-absorbance by diatom populations from the Weddell–Scotia Confluence. Antarctic J. U.S. **29:** 266–267.

NELSON, D. M., AND W. O. SMITH. 1991. Sverdrup revisited: Critical depths, maximum chlorophyll levels and the control of Southern Ocean productivity by the irradiance-mixing regime. Limnol. Oceanogr. **36:** 1650–1661.

———, ———, L. I. GORDON, AND B. A. HUBER. 1987. Spring distributions of density, nutrients and phytoplankton biomass in the ice edge zone of the Weddell–Scotia Sea. J. Geophys. Res. **92:** 7181–7190.

PLATT, T., C. L. GALLEGOS, AND W. G. HARRISON. 1980. Photoinhibition of photosynthesis in natural assemblages of marine phytoplankton. J. Mar. Res. **38:** 687–701.

PRÉZELIN, B. B., N. B. BOUCHER, AND R. C. SMITH. 1994. Marine primary production under the influence of the Antarctic ozone hole: Icecolors '90, p. 159–186. *In* C. S. Weiler and P. A. Penhale [eds.], Ultraviolet radiation and biological research in Antarctica. AGU.

QUAITE, F. E., B. M. SUTHERLAND, AND J. C. SUTHERLAND. 1992. Action spectrum for DNA damage in alfalfa lowers predicted impact of ozone depletion. Nature **358:** 576–578.

RIDOUT, P. S., AND R. J. MORRIS. 1985. Short-term variations in the pigment composition of a spring phytoplankton bloom from an enclosed experimental ecosystem. Mar. Biol. **87:** 7–11.

RUNDEL, R. D. 1983. Action spectra and estimation of biologically effective UV radiation. Physiol. Plant. **58:** 360–366.

SMITH, R. C., K. S. BAKER, O. HOLM-HANSEN, AND R. S. OLSON. 1980. Photoinhibition of photosynthesis in natural waters. Photochem. Photobiol. **31:** 585–592.

———, AND J. J. CULLEN. 1995. Effects of UV radiation on phytoplankton. Rev. Geophys. **33:** 1211–1223.

SMITH, W. O., AND D. M. NELSON. 1986. Importance of ice edge phytoplankton production in the Southern Ocean. Bioscience **36:** 251–257.

———, AND OTHERS. 1992. Ozone depletion: Ultraviolet radiation and phytoplankton biology in Antarctic waters. Science **255:** 952–959.

SOLOMON, S. 1988. The mystery of the Antarctic ozone "hole." Rev. Geophys. **26:** 131–148.

SULLIVAN, C. W., C. R. MCCLAIN, J. C. COMISO, AND W. O. SMITH. 1988. Phytoplankton standing crops within an Antarctic ice edge assessed by satellite remote sensing. J. Geophys. Res. **93:** 12487–12498.

VERNET, M., E. A. BRODY, O. HOLM-HANSEN, AND B. G. MITCHELL. 1994. The response of Antarctic phytoplankton to ultraviolet radiation: Absorption, photosynthesis, and taxonomic composition, p. 143–158. *In* C. S. Weiler and P. A. Penhale [eds.], Ultraviolet radiation and biological research in Antarctica. AGU.

VINCENT, W. F., AND S. ROY. 1993. Solar ultraviolet-B radiation and aquatic primary production: Damage, protection and recovery. Environ. Rev. **1:** 1–12.

WEBB, W. L., M. NEWTON, AND D. STARR. 1974. Carbon dioxide exchange of *Alnus rubra.* A mathematical model. Oecologia (Berlin) **17:** 281–291.

WMO. 1995. Scientific assessment of ozone depletion: 1994. World Meteorological Organization, Geneva.

Received: 2 January 1997
Accepted: 12 November 1997